AMERICAN SOCIETY FOR MICROBIOLOGY | Applied and Environmental Microbiology®

PLANT MICROBIOLOGY

A Novel Regulatory Pathway for K^+ Uptake in the Legume Symbiont *Azorhizobium caulinodans* in Which TrkJ Represses the *kdpFABC* Operon at High Extracellular K^+ Concentrations

Lowela Siarot,[a] Hiroki Toyazaki,[a] Makoto Hidaka,[b] Keigo Kurumisawa,[c] Tomoki Hirakawa,[c] Kengo Morohashi,[c] Toshihiro Aono[a]

Biotechnology Research Center, The University of Tokyo, Tokyo, Japan[a]; Graduate School of Agricultural and Life Sciences, The University of Tokyo, Tokyo, Japan[b]; Faculty of Science and Technology, Tokyo University of Science, Tokyo, Japan[c]

ABSTRACT Bacteria have multiple K^+ uptake systems. *Escherichia coli*, for example, has three types of K^+ uptake systems, which include the low-K^+-inducible KdpFABC system and two constitutive systems, Trk (TrkAG and TrkAH) and Kup. *Azorhizobium caulinodans* ORS571, a rhizobium that forms nitrogen-fixing nodules on the stems and roots of *Sesbania rostrata*, also has three types of K^+ uptake systems. Through phylogenetic analysis, we found that *A. caulinodans* has two genes homologous to *trkG* and *trkH*, designated *trkI* and *trkJ*. We also found that *trkI* is adjacent to *trkA* in the genome and these two genes are transcribed as an operon; however, *trkJ* is present at a distinct locus. Our results demonstrated that *trkAI*, *trkJ*, and *kup* were expressed in the wild-type stem nodules, whereas *kdpFABC* was not. Interestingly, Δ*kup* and Δ*kup* Δ*kdpA* mutants formed Fix^- nodules, while the Δ*kup* Δ*trkA* Δ*trkI* Δ*trkJ* mutant formed Fix^+ nodules, suggesting that with the additional deletion of Trk system genes in the Δ*kup* mutant, Fix^+ nodule phenotypes were recovered. *kdpFABC* of the Δ*kup* Δ*trkJ* mutant was expressed in stem nodules, but not in the free-living state, under high-K^+ conditions. However, *kdpFABC* of the Δ*kup* Δ*trkA* Δ*trkI* Δ*trkJ* mutant was highly expressed even under high-K^+ conditions. The cytoplasmic K^+ levels in the Δ*kup* Δ*trkA* Δ*trkI* mutant, which did not express *kdpFABC* under high-K^+ conditions, were markedly lower than those in the Δ*kup* Δ*trkA* Δ*trkI* Δ*trkJ* mutant. Taking all these results into consideration, we propose that TrkJ is involved in the repression of *kdpFABC* in response to high external K^+ concentrations and that the TrkAI system is unable to function in stem nodules.

IMPORTANCE K^+ is a major cytoplasmic cation in prokaryotic and eukaryotic cells. Bacteria have multiple K^+ uptake systems to control the cytoplasmic K^+ levels. In many bacteria, the K^+ uptake system KdpFABC is expressed under low-K^+ conditions. For years, many researchers have argued over how bacteria sense K^+ concentrations. Although KdpD of *Escherichia coli* is known to sense both cytoplasmic and extracellular K^+ concentrations, the detailed mechanism of K^+ sensing is still unclear. In this study, we propose that the transmembrane TrkJ protein of *Azorhizobium caulinodans* acts as a sensor for the extracellular K^+ concentration and that high extracellular K^+ concentrations repress the expression of KdpFABC via TrkJ.

KEYWORDS potassium transport, rhizobium, symbiosis

Azorhizobium caulinodans ORS571 is a microsymbiont of the water-tolerant tropical legume *Sesbania rostrata* (1–3), where it forms N_2-fixing nodules on the stems and roots. A previous transposon mutagenesis study on the rhizobial factors involved in

Received 27 May 2017 **Accepted** 28 July 2017

Accepted manuscript posted online 4 August 2017

Citation Siarot L, Toyazaki H, Hidaka M, Kurumisawa K, Hirakawa T, Morohashi K, Aono T. 2017. A novel regulatory pathway for K^+ uptake in the legume symbiont *Azorhizobium caulinodans* in which TrkJ represses the *kdpFABC* operon at high extracellular K^+ concentrations. Appl Environ Microbiol 83:e01197-17. https://doi.org/10.1128/AEM.01197-17.

Editor Maia Kivisaar, University of Tartu

Address correspondence to Toshihiro Aono, uaono@mail.ecc.u-tokyo.ac.jp.

normal stem nodule development showed that *A. caulinodans* mutants with disruptions of *kup*, the gene encoding the K^+ uptake system Kup, formed stem nodules lacking N_2-fixing activity (4).

Generally, there are four K^+ transport systems found in bacteria: the Trk, Ktr, Kup, and Kdp systems. The Trk system is a major constitutive K^+ uptake system found in most bacterial species and in several archaeal species. It has a moderate affinity for K^+ in the vicinity of 1 mM (5) and probably takes up K^+ in symport with a proton (5, 6). It is a multicomponent complex that consists of a K^+-translocating subunit, either transmembrane protein TrkG or TrkH, and a cytoplasmic membrane surface protein, TrkA, which carries the NAD^+ binding site that is necessary for the activity of the Trk system (6, 7). For Trk function in *Escherichia coli*, either of the homologous genes *trkG* or *trkH* suffices, but the catalytic domain gene *trkA* is essential (8, 9). The specificity of the system depends on which of these two membrane-spanning components is involved (10). The *trkH*-dependent transport requires an additional gene, *trkE*, which encodes an ATP-binding protein (8, 9), whereas *trkG*-dependent transport requires ATP (5, 11) yet only partially requires TrkE (8).

The Ktr system is similar to the Trk system and is found in many bacteria, but not in archaea (5). It consists of two components, KtrA and KtrB, which are distantly related to TrkA and TrkH, respectively (5). KtrA is about half the size of TrkA, with a region that shares sequence homology with the NAD^+-binding domain of some dehydrogenases (5).

The Kup system, which has a modest affinity for K^+, is a constitutively expressed type of K^+ uptake system present in some bacteria, but its activity is inhibited at elevated osmolarity (5). The Kup system protein is encoded by a single gene and is composed of two domains: an integral membrane domain that has 12 putative transmembrane spanners and a hydrophilic C-terminal domain (11).

The Kdp system, which consists of four subunits encoded by the *kdpFABC* operon, has a high affinity for K^+. It is the only K^+ uptake system that is induced by environmental conditions such as a decrease in turgor pressure or low K^+ concentrations (5, 6, 12). KdpA is a K^+-binding and transport protein and is highly hydrophobic, with 10 membrane-spanning segments (13). KdpB is the homologue of other P-type ATPases and contains a highly conserved phosphorylation site. KdpC is presumed to have only a single membrane-spanning segment and is involved in linking KdpA and KdpB together, serving to assemble and stabilize the KdpFABC complex (13, 14). KdpA, KdpB, and KdpC are sufficient to form a functional transport complex (15, 16), but all three subunits are required for normal Kdp activity (13). KdpF, which in *E. coli* is a small peptide consisting of 29 amino acids, is dispensable but important for the stability of the Kdp complex (17, 18). The expression of the *kdpFABC* operon is positively controlled by a two-component KdpDE system in response to low K^+ concentrations (19).

In the genome of *A. caulinodans*, three K^+ uptake systems, Kdp, Trk, and Kup, have been identified, and *kup* mutants were observed to form dysfunctional stem nodules as described above. This raised the hypothesis that the Kup system of *A. caulinodans* plays an essential role in stem nodules that could not be complemented by the other K^+ uptake systems. To test this hypothesis, we studied the contribution of each of the K^+ uptake systems to nodule formation by constructing deletion mutants of each gene and analyzing the expression patterns of the genes.

RESULTS

Genetic organization of the K^+ uptake system genes in *A. caulinodans*. Maps of the K^+ uptake system genes of *A. caulinodans* ORS571 are shown in Fig. 1. The similarity of the proteins encoded by these genes to those of *E. coli* or other bacteria are listed in Table S1 in the supplemental material.

The AZC_4041 locus tag on the genome was named *kup*. Reverse transcription-PCR (RT-PCR) analysis revealed that *kup* was transcribed in a monocistronic manner (see Fig. S1 in the supplemental material).

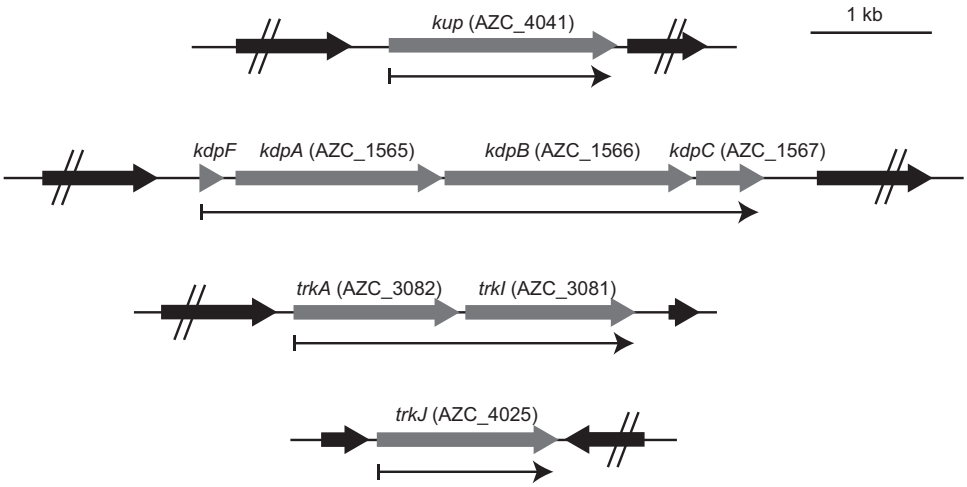

FIG 1 Genetic organization of the K^+ uptake system genes in *A. caulinodans* ORS571. Thin arrows below each map indicate transcription units of K^+ uptake system genes.

The AZC_1565, AZC_1566, and AZC_1567 locus tags, which are adjacent in the genome, were named *kdpA*, *kdpB*, and *kdpC*, respectively. A small open reading frame was found in the upstream region of *kdpA* and designated *kdpF*, but the locus tag of this gene was not assigned. The KdpF of *A. caulinodans* is not identical to that of *E. coli* but to that of putative KdpF proteins of species belonging to the *Alphaproteobacteria* (Table S1). The gene cluster of *kdpFABC* was transcribed as an operon (Fig. S1).

The AZC_3082 gene was named *trkA*. Two genes homologous to *trkG* and *-H* were identified in the genome of *A. caulinodans*. One is AZC_3081, which is located downstream of *trkA*, and the other is AZC_4025. A phylogenetic analysis based on the putative amino acid sequences of the bacterial proteins homologous to TrkG and -H revealed that the AZC_3081 protein belongs to a cluster that includes TrkI of *Halomonas elongata* (20) and that the AZC_4025 protein belongs to a new cluster consisting of proteins from *Alphaproteobacteria*, which is a cluster different from those that consist of TrkG, TrkH, and TrkI proteins (Fig. 2). Thus, AZC_3081 and AZC_4025 were named *trkI* and *trkJ*, respectively. The gene cluster of *trkAI* was transcribed as an operon, whereas *trkJ* was transcribed in a monocistronic manner (Fig. S1).

Transcriptional activities of K^+ uptake system genes. To investigate the transcriptional activities of *kup*, *kdpFABC*, *trkAI*, and *trkJ*, we constructed strains harboring a transcriptional fusion of *lacZ* with *kup*, *kdpF*, *trkA*, or *trkJ*, and these were designated the wild-type (WT) *kup-lacZ*, *kdpF-lacZ*, *trkA-lacZ*, and *trkJ-lacZ* strains, respectively. These strains were grown at various K^+ concentrations (0.05 to 5 mM), and their β-galactosidase activities were measured (Fig. 3A). Consistent with its regulation in other bacteria, the expression of *kdpFABC* was induced under low-K^+ conditions, and *kup*, *trkAI*, and *trkJ* were constitutively expressed irrespective of the environmental K^+ concentration. To investigate the transcriptional activities of these genes/operons in the symbiotic state, we stained stem nodules formed after inoculation with these strains with 5-bromo-4-chloro-3-indolyl-β-D-galactopyranoside (X-Gal) (Fig. 3B). We detected the transcriptional activities of *kup*, *trkAI*, and *trkJ* in the infected regions of the stem nodules. However, *kdpFABC* was not expressed in the infected regions of the stem nodules, suggesting that stem nodules are abundant under K^+ conditions.

Phenotypes of stem nodules formed by mutant strains with deletions of K^+ uptake system genes. We constructed a series of mutants with deletions of K^+ uptake system genes as described in Materials and Methods. We first observed the stem nodules formed by the Δ*kup*, Δ*kdpA*, Δ*trkA* Δ*trkI* Δ*trkJ*, Δ*kdpA* Δ*trkA* Δ*trkI* Δ*trkJ*, Δ*kup* Δ*trkA* Δ*trkI* Δ*trkJ*, and Δ*kup* Δ*kdpA* strains and measured acetylene reduction activities (ARAs), which

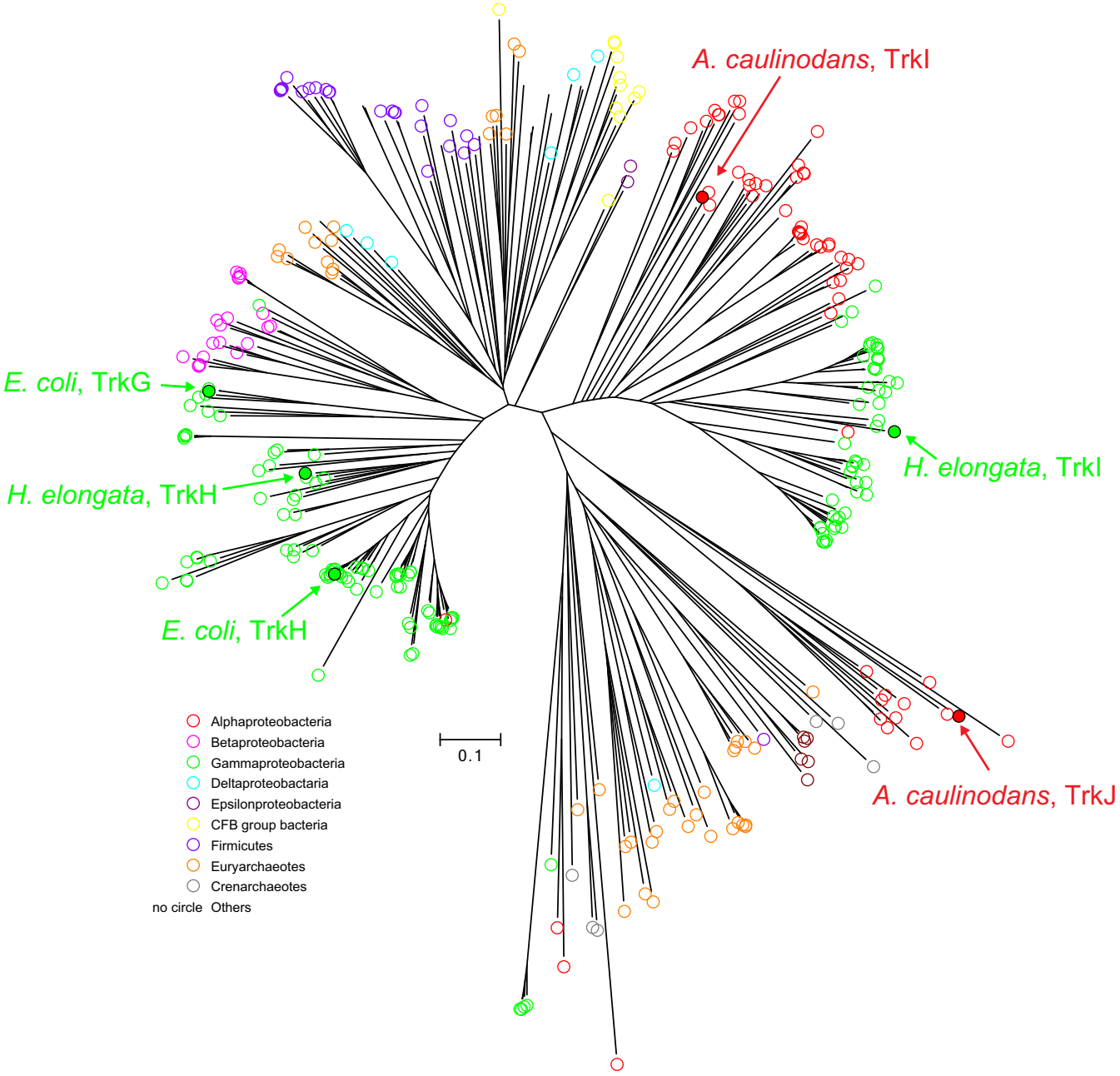

FIG 2 Phylogenetic relationships among TrkG and -H family proteins. Amino acid sequences were obtained by a BLASTp search on the NCBI server using the AZC_3081 protein as a query, and phylogenetic analyses were performed using MUSCLE. The amino acid sequences used in this analysis are listed in Data Set S1 in the supplemental material. Colored circles indicate the taxa of bacteria that possess each TrkG and -H family protein.

reflect nitrogen fixation activities (Fig. 4). The stem nodules formed by the Δ*kup* mutant showed Fix$^-$ phenotypes, characterized by white inner regions and limited nitrogen fixation activities; while the Δ*kdpA*, Δ*trkA* Δ*trkI* Δ*trkJ* and Δ*kdpA* Δ*trkA* Δ*trkI* Δ*trkJ* mutants formed Fix$^+$ stem nodules showing pink inner regions and high nitrogen-fixing activities. These results suggest that the Kup system is an essential K^+ uptake system to maintain stem nodules and that the Trk and Kdp systems are not required for normal nodule formation. Interestingly, the Δ*kup* Δ*trkA* Δ*trkI* Δ*trkJ* mutant rather than the Δ*kup* Δ*kdpA* mutant formed Fix$^+$ stem nodules, indicating that the Fix$^-$ phenotype of the stem nodules caused by *kup* deletion was recovered by the additional deletion of the Trk system genes.

To determine which genes among *trkA*, *trkI*, and *trkJ* contribute to the reversion of the Fix$^-$ phenotype caused by the *kup* deletion, we observed the stem nodules formed

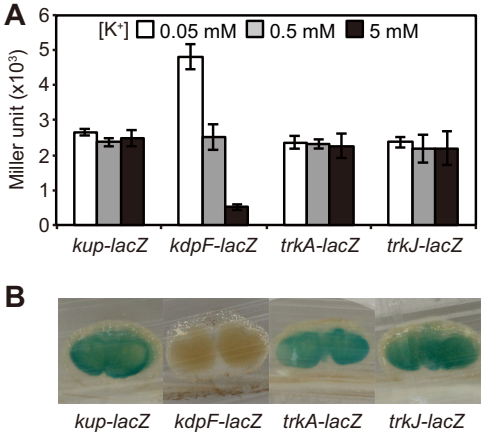

FIG 3 Transcriptional activities of K^+ uptake system genes in the free-living and symbiotic states. (A) Effect of extracellular K^+ concentration on the expression of *kup*, *kdpFABC*, *trkAI*, and *trkJ*. The WT *kup-lacZ*, *kdpF-lacZ*, *trkA-lacZ*, and *trkJ-lacZ* strains were grown for 4 h under 0.05, 0.5, and 5 mM K^+ conditions, and the β-galactosidase activities of these strains were measured. Data are presented as the means ± standard deviations from three replicate cultures. (B) Expression of *kup*, *kdpFABC*, *trkAI*, and *trkJ* in stem nodules. Stem nodules formed by the indicated strains were sliced at 12 days postinoculation (dpi), and the β-galactosidase activity was detected by staining with X-Gal.

by *kup* mutants with additional deletions of *trkA*, *trkI*, and/or *trkJ* and their combinations (Fig. 5A and B). The mutants with common deletions of *kup* and *trkJ* (i.e., the Δ*kup* Δ*trkJ*, Δ*kup* Δ*trkA* Δ*trkJ*, Δ*kup* Δ*trkI* Δ*trkJ*, and Δ*kup* Δ*trkA* Δ*trkI* Δ*trkJ* strains) formed Fix^+ stem nodules, regardless of *trkA* and *trkI* deletion. However, the Δ*kup* Δ*kdpA* Δ*trkJ* mutant formed Fix^- stem nodules, although it has a common deletion of *kup* and *trkJ*. Microscopic analysis was performed to observe in detail the phenotypes of the stem nodules formed by these mutants (Fig. 5C). In the stem nodules formed by the WT and Δ*kup* Δ*trkJ* strains, we observed that plant host cells were filled with bacterial cells. However, those formed by the Δ*kup* and Δ*kup* Δ*kdpA* Δ*trkJ* mutants have very low numbers of bacterial cells inside the plant host cells, suggesting that these mutant strains had difficulty surviving in the plant host cells. Based on these results, we

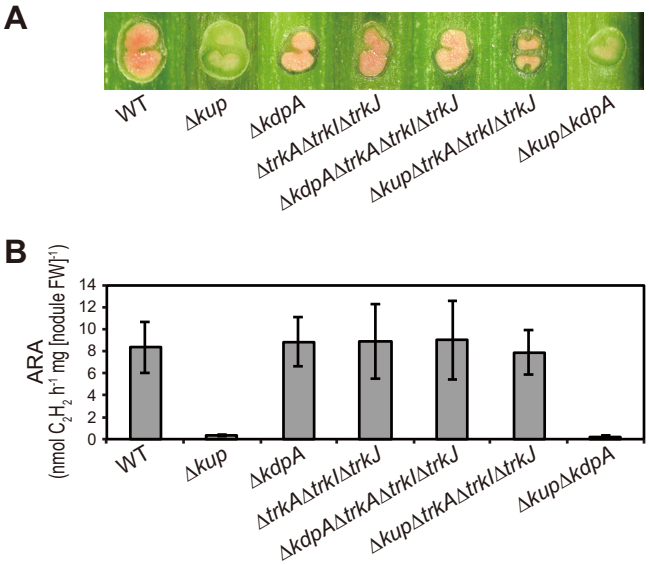

FIG 4 Phenotypes of stem nodules formed by mutant strains with deletion of K^+ uptake system genes. Stem nodules formed by the indicated strains were observed at 12 dpi. (A) Images of the hand-cut stem nodules. (B) N_2 fixation activities of the stem nodules as assessed by ARAs. Data are presented as the means ± standard deviations from five separate plants. FW, fresh weight.

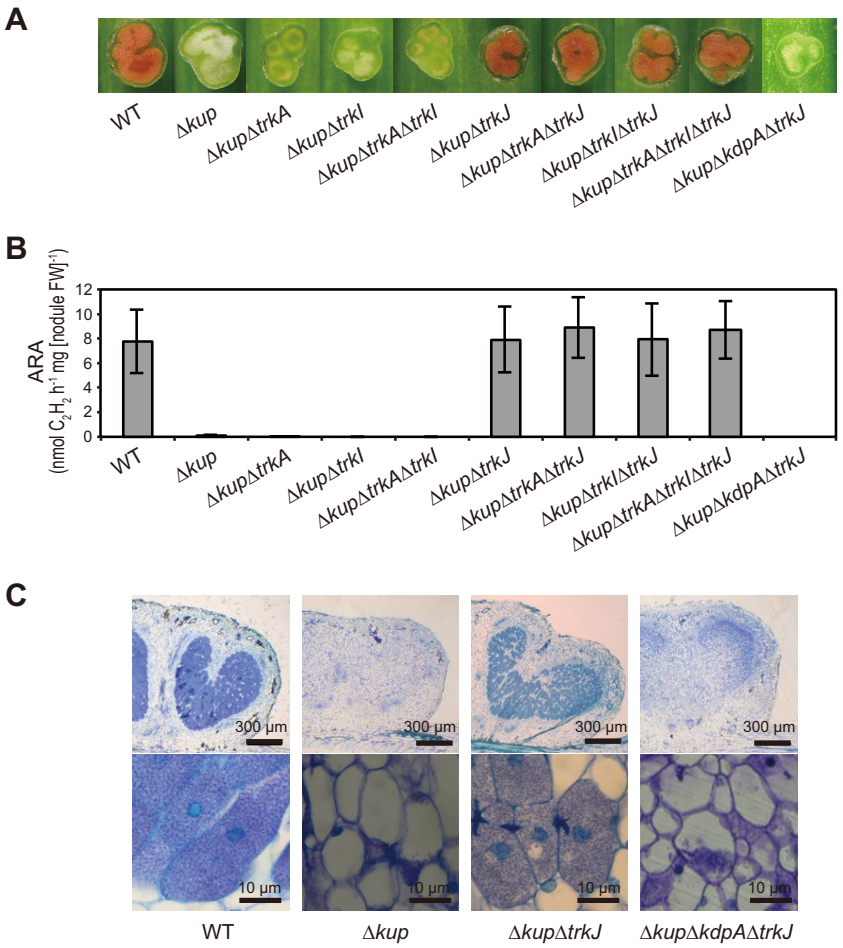

FIG 5 Effect of *trkJ* deletion on the Fix$^-$ phenotype caused by *kup* deletion. Stem nodules formed by the indicated strains were observed at 12 dpi. (A) Images of the hand-cut stem nodules. (B) ARAs of the stem nodules. Data are presented as the means ± standard deviations from five separate plants. FW, fresh weight. (C) Optical microscopy observations of the stem nodules. Stem nodules were longitudinally sectioned and stained with toluidine blue O.

hypothesized that simultaneous deletion of *kup* and *trkJ* induces high expression of the *kdpFABC* operon. Furthermore, we hypothesized that the TrkAI uptake system cannot function in the symbiotic state. To test these hypotheses, we conducted expression analyses of the *kdpFABC* operon.

Effects of simultaneous deletion of *kup* and *trkA*, *-I*, and/or *-J* on the transcriptional activity of *kdpFABC*. The *kdpF-lacZ* fusion was introduced into the mutants with deletions of *kup* and *trk* genes. The resultant mutants were grown under various K^+ conditions, and their β-galactosidase activities were measured to investigate the transcriptional activity of *kdpFABC* (Fig. 6A). In the mutants with simultaneous deletions of *kup*, *trkA* and/or *-I*, and *trkJ* (i.e., the Δ*kup* Δ*trkA* Δ*trkJ* *kdpF-lacZ*, Δ*kup* Δ*trkI* Δ*trkJ* *kdpF-lacZ*, and Δ*kup*Δ *trkA* Δ*trkI* Δ*trkJ* *kdpF-lacZ* mutants), the expression levels of *kdpFABC* were high even under high-K^+ conditions. However, *kdpFABC* was not induced in the Δ*kup* Δ*trkJ* *kdpF-lacZ* mutant under high-K^+ conditions but under low-K^+ conditions instead. These results revealed that simultaneous deletion of *kup*, *trkJ*, and of *trkA* and/or *trkI* induced a high level of expression of *kdpFABC* even under high-K^+ conditions. To determine the reason why the Δ*kup* Δ*trkJ* mutant could form Fix$^+$ stem nodules, we observed the stem nodules formed by the Δ*kup* Δ*trkJ* *kdpF-lacZ* mutant. We detected high expression of *kdpFABC* in the stem nodules formed by the Δ*kup* Δ*trkJ* *kdpF-lacZ* mutant, like those observed in the Δ*kup* Δ*trkA* Δ*trkI* Δ*trkJ* *kdpF-lacZ* mutant

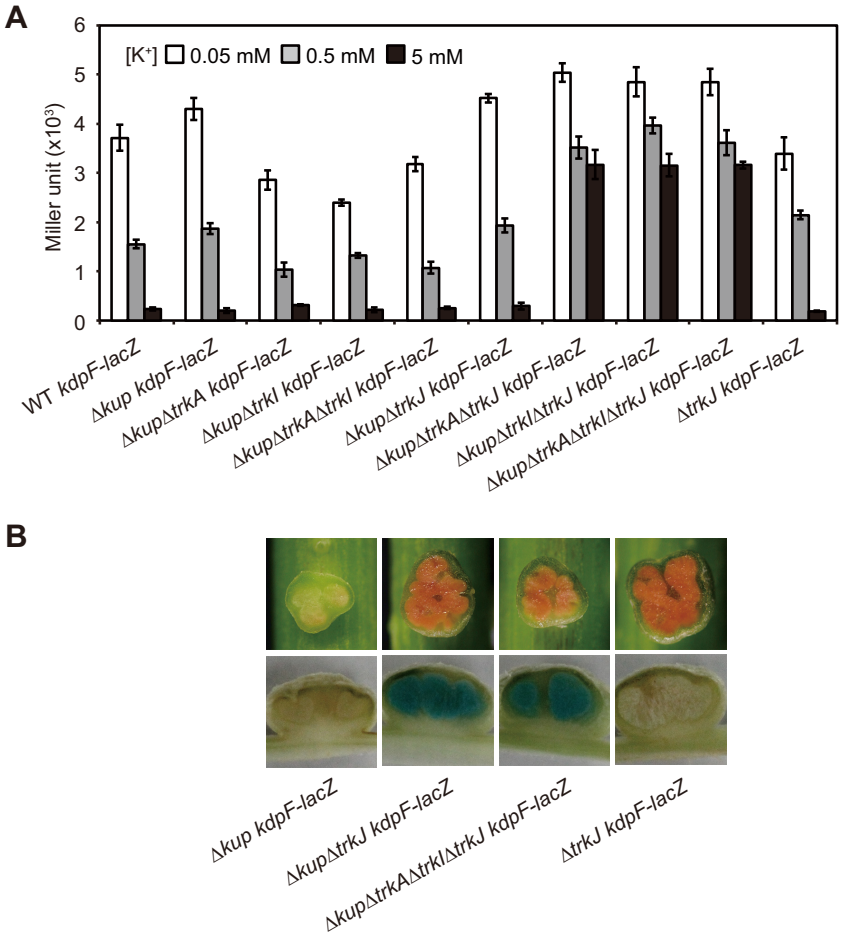

FIG 6 Effects of simultaneous deletion of *kup* and *trkA*, *-I*, and/or *-J* on the transcriptional activity of *kdpFABC*. (A) Transcriptional activity of *kdpFABC* in the indicated strains in the free-living state under various K^+ conditions. The strains were grown for 4 h under 0.05, 0.5, and 5 mM K^+ conditions, and their β-galactosidase activities were measured. Data are presented as the means ± standard deviations from three replicate cultures. (B) Expression of *kdpFABC* in stem nodules. The stem nodules formed by the indicated strains were observed at 12 dpi (upper panels), and β-galactosidase activity was detected by staining with X-Gal (lower panels).

(Fig. 6B). These results indicate that the TrkAI system cannot function in the symbiotic state, as hypothesized above.

Cytoplasmic K^+ content and growth in the free-living state. To investigate the relationships of *kdpFABC* expression, cytoplasmic K^+ contents, and the growth of the mutants with deletions of *kup* and *trkA*, *-I*, and/or *-J*, we grew a series of mutants (shown in Fig. 5) under various K^+ conditions (Fig. 7). Lower cytoplasmic K^+ contents were observed in the Δ*kup* Δ*trkA*, Δ*kup* Δ*trkI*, and Δ*kup* Δ*trkA* Δ*trkI* mutants under higher extracellular K^+ conditions (Fig. 7A). Furthermore, the cytoplasmic K^+ contents of these mutants under 0.5 and 5 mM K^+ conditions were much lower than those of other mutants. The growth of these mutants was also inhibited under 0.5 and 5 mM K^+ conditions (Fig. 7B). These results suggest that the mutants with common deletion of *kup* and of *trkA*, *trkI*, or both (Δ*kup* Δ*trkA*, Δ*kup* Δ*trkI*, and Δ*kup* Δ*trkA* Δ*trkI* strains) were unable to effectively import K^+ since these mutants lacked Kup and TrkAI, and even if the KdpFABC system is present, it was not expressed. The low levels of cytoplasmic K^+ in these mutants were rectified by additional deletion of *trkJ*; the Δ*kup* Δ*trkA* Δ*trkJ*, Δ*kup* Δ*trkI* Δ*trkJ*, and Δ*kup* Δ*trkA* Δ*trkI* Δ*trkJ* mutants contained higher cytoplasmic K^+ levels than the Δ*kup* Δ*trkA*, Δ*kup* Δ*trkI*, and Δ*kup* Δ*trkA* Δ*trkI* mutants under 0.5 and 5 mM K^+ conditions. Furthermore, the former mutants lacking *trkJ* grew better than the latter mutants possesing *trkJ*.

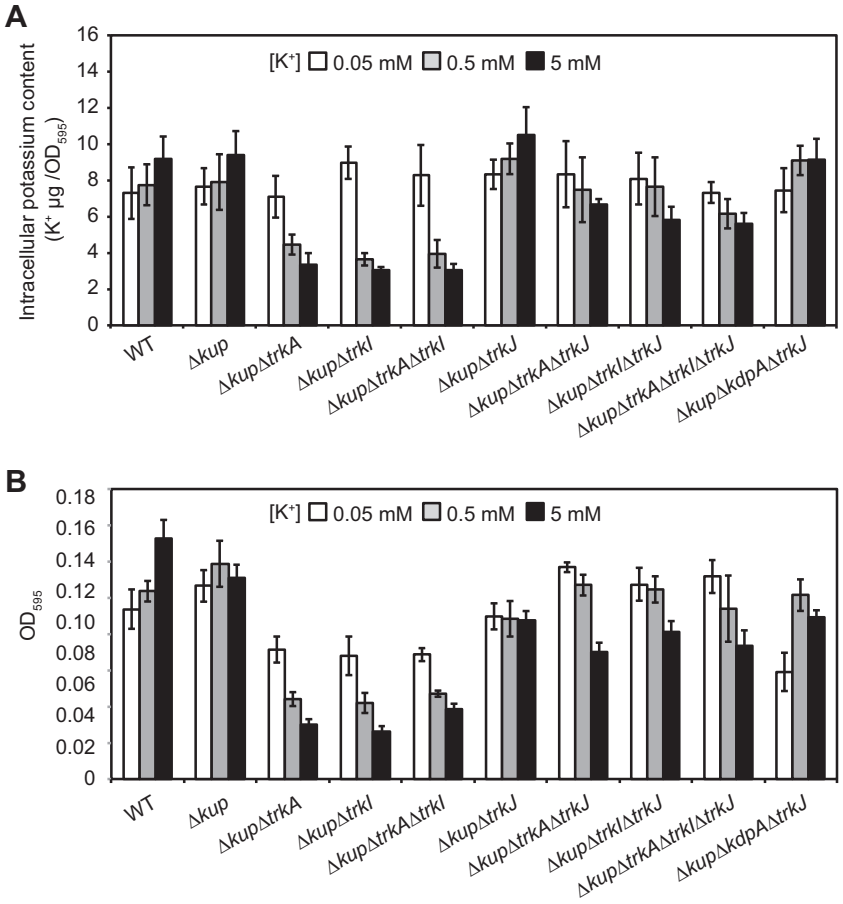

FIG 7 Cytoplasmic K^+ content and growth in the free-living state. (A) Cytoplasmic K^+ content of the indicated strains grown under various K^+ conditions. Bacterial cells grown for 4 h under 0.05, 0.5, and 5 mM K^+ conditions were collected, washed with 50 mM NaCl, and then suspended in pure water. These cell suspensions were boiled, and the extracted K^+ was measured. Total extracted K^+ was normalized to the OD_{595} of each cell suspension. (B) Growth of the indicated strains under various K^+ conditions. Each strain was suspended in medium with 0.05, 0.5, and 5 mM K^+ to an OD_{600} of 0.05 and incubated for 16 h with shaking. After incubation, the OD_{595} of each culture was measured using a 96-well microplate reader. In panels A and B, data are presented as the means ± standard deviations from three replicate cultures.

DISCUSSION

The present study provides evidence of a novel pathway for the regulatory mechanism of K^+ uptake systems in a plant symbiotic bacterium. Here, we propose that TrkJ, a TrkG and/or TrkH homologue, acts as a repressor for the expression of *kdpFABC*, the operon encoding the high-affinity K^+ uptake KdpFABC system, probably via sensing a high extracellular K^+ concentration. We also propose that the TrkAI system cannot function in the symbiotic state (Fig. 8A).

These propositions are manifested in the phenotypes of the mutants in the symbiotic and free-living states. The Δ*kup* mutant in the symbiotic state (Fig. 8B) is unable to import K^+ via the TrkAI and Kup systems because the former cannot function in the symbiotic state, and the latter is lacking; it is also unable to import K^+ via the KdpFABC system because *kdpFABC* expression is repressed—most probably via TrkJ—in response to high extracellular K^+ concentrations. Hence, the Δ*kup* mutant could hardly import K^+ in the stem nodules and eventually could barely survive there, resulting in Fix^- stem nodules. On the contrary, the Δ*kup* Δ*trkJ* mutant in the symbiotic state (Fig. 8C) may import K^+ via the KdpFABC system, which is expressed in response to low cytoplasmic K^+ concentrations, because the mutant is defective in TrkJ-mediated repression of *kdpFABC* expression. Thus, the Δ*kup* Δ*trkJ* mutant can avoid critically low cytoplasmic

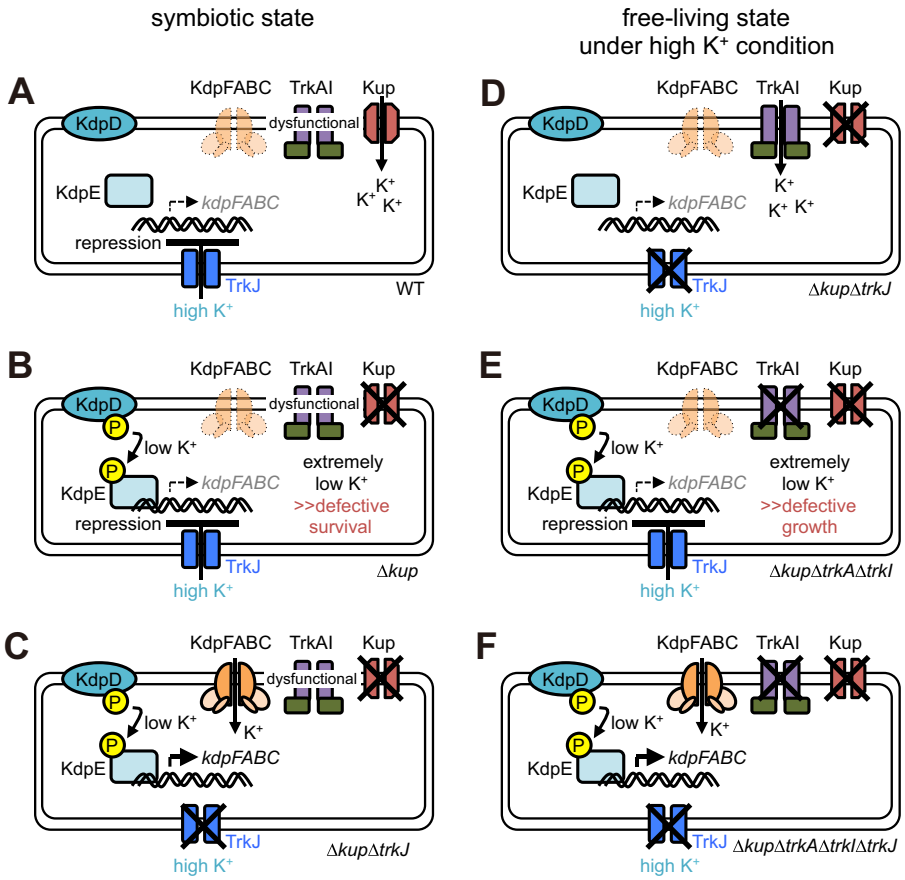

FIG 8 Model for regulation of the TrkAI and KdpFABC systems. The findings of this study strongly suggest that the TrkAI system is unable to function in the symbiotic state and that *kdpFABC* expression is repressed by high extracellular K^+ concentrations via TrkJ. The details are described in the Discussion section in the main text.

K^+ concentrations and form Fix^+ stem nodules. In the free-living state, this Δ*kup* Δ*trkJ* mutant does not express *kdpFABC* under high-K^+ conditions because it can import sufficient K^+ via the TrkAI system (Fig. 8D). The Δ*kup* Δ*trkA* Δ*trkI* mutant in the free-living state (Fig. 8E) likely imports little K^+ under high-K^+ conditions because it lacks the TrkAI and Kup systems and is unable to express *kdpFABC* due to TrkJ-mediated repression. Thus, this mutant is defective in growth under high-K^+ conditions. It grows better under low-K^+ conditions than under high-K^+ conditions because the TrkJ-mediated repression of *kdpFABC* expression could be prevented under low-K^+ conditions and because it is able to import K^+ via the KdpFABC system. The Δ*kup* Δ*trkA* Δ*trkI* Δ*trkJ* mutant in the free-living state (Fig. 8F) is defective in K^+ uptake via the TrkAI and Kup systems under high-K^+ conditions but avoids critically low cytoplasmic K^+ concentrations by expressing the KdpFABC system because this mutant lacks the TrkJ-mediated repression system of *kdpFABC* expression.

Generally, transcription of the *kdpFABC* operon is positively controlled by the two-component system KdpDE in response to low K^+ concentrations. The *E. coli* KdpD consists of a cytoplasmic N-terminal domain and a cytoplasmic C-terminal domain (kinase domain) interconnected by four transmembrane segments (21). In the case of *E. coli*, it has been proposed that the cytoplasmic C-terminal domain of KdpD senses intracellular K^+ (22) and that the periplasmic loops of KdpD sense extracellular K^+ (23).

For years, KdpDE has been thought to be the sole regulatory system of the *kdpFABC* operon. However, this study provides insight into the possible presence of inhibitors that interact with KdpDE or the presence of a regulatory system other than KdpDE that

controls the expression of *kdpFABC*. Whether TrkJ is a separate regulatory system or just a protein inhibitor interfering with the KdpDE system, elucidation of the structure of TrkJ of *A. caulinodans* would clarify the nature of its involvement in *kdpFABC* expression. The possible interactions of TrkJ with the histidine kinase KdpD or the response regulator KdpE, which controls the expression of the *kdpFABC* operon in response to K^+, warrant further investigation.

In relation to the proposed mechanism of TrkJ-mediated control of the expression of *kdpFABC*, a connection between the Trk and Kdp systems has previously been reported. The Trk and Kdp systems are linked via a clever regulatory mechanism, the enzyme IIA^{Ntr} ($EIIA^{Ntr}$) of the nitrogen-metabolic phosphotransferase system. This enzyme directly interacts with KdpD, as well as with TrkA, thereby regulating *kdpFABC* expression and inhibiting Trk, respectively (24, 25). The dephosphorylated form of $EIIA^{Ntr}$ binds and inhibits TrkA activity (24); it also independently interacts with the sensor kinase KdpD and stimulates kinase activity, resulting in increased levels of the phosphorylated response regulator KdpE (25). Although the binding of dephosphorylated $EIIA^{Ntr}$ to TrkA to inhibit Trk activity is independent of the $EIIA^{Ntr}$-mediated regulatory mechanism of *kdpFABC* expression (25), it is noteworthy that both activities occur as consequences and subsequent steps of a common event—the formation of dephosphorylated $EIIA^{Ntr}$. This supports our findings that there is a link between the Trk and Kdp systems. This also supports our hypothesis that TrkJ might interact directly or indirectly with the KdpDE regulatory system and that this interaction could lead to the repression of *kdpFABC* expression. Furthermore, it would be interesting whether or not $EIIA^{Ntr}$ is involved in the inactivation of the TrkAI system in the stem nodules.

Moreover, there is a need to verify the ubiquity of the novel regulatory mechanism of K^+ uptake systems. The results of the phylogenetic analyses of TrkA/G family proteins suggest that TrkJ-mediated repression in response to extracellular K^+ is limited to *Alphaproteobacteria*. Furthermore, this regulatory system might be specific to some species of *Alphaproteobacteria* because not all of the *Alphaproteobacteria* possess TrkJ homologues.

MATERIALS AND METHODS

Bacterial strains and media. The bacterial strains used in this study are listed in Table 1. *A. caulinodans* ORS571, the WT strain, and its derivatives were grown at 38°C in either tryptone-yeast extract (TY) medium (26) supplemented with 15 mM KCl or in synthetic medium supplemented with 0.05, 0.5, or 5 mM KCl. The synthetic medium is composed of 10 mM NH_4Cl, 10 mM sodium phosphate (pH 7.0), 50 mM disodium succinate, 100 mg liter^{-1} $MgSO_4 \cdot 7H_2O$, 50 mg liter^{-1} NaCl, 40 mg liter^{-1} $CaCl_2 \cdot 2H_2O$, 5.4 mg liter^{-1} $FeCl_3 \cdot 6H_2O$, 5 mg liter^{-1} $Na_2MoO_4 \cdot 2H_2O$, 2 mg liter^{-1} biotin, 4 mg liter^{-1} nicotinic acid, and 4 mg liter^{-1} pantothenic acid. Inoculation of *A. caulinodans* strains into the synthetic medium supplemented with KCl was carried out as follows. Bacterial cells grown overnight in TY medium with 15 mM KCl were collected by centrifugation and washed twice with KCl-free synthetic medium. The washed bacterial cells were suspended in KCl-free synthetic medium, and the cell suspensions were diluted with equal amounts of synthetic medium supplemented with 0.1, 1, or 10 mM KCl. The final concentrations of KCl were 0.05, 0.5, and 5 mM. The cultures of each strain were then incubated with shaking.

Construction of bacterial strains. The plasmids and primers used for strain construction are listed in Tables 1 and 2, respectively. Plasmids for gene deletion were constructed by splicing by overhang extension (SOE) PCR (27). The genomic DNA isolated from the WT strain was used as a template in each first-round PCR. To construct the plasmid for *kup* deletion, fragments containing the 5′ end and 3′ end of *kup* were amplified by PCR, using primer pairs Acp16-Acp17 and Acp18-Acp19, respectively. Acp17 contains the complementary sequence of Acp18, and the two amplified fragments were integrated by a second PCR using Acp16 and Acp19. The integrated fragment was cloned into EcoRI and BamHI sites in pK18*mobsac*B (28), which is a suicide vector allowing sucrose selection for vector loss. The resulting plasmid was designated pTAC3. Similarly, the plasmids for the deletion of *kdpA*, *trkAI*, *trkA*, *trkI*, and *trkJ* were constructed using the primers listed in Table 2 and designated pTAC39, pTAC40, pTAC110, pTAC111, and pTAC41, respectively. These plasmids were conjugated into WT and mutant strains via *E. coli* S17-1(λpir) (29), and gene deletions were introduced by allelic exchange.

In order to construct *kup-lacZ*, *kdpF-lacZ*, *trkA-lacZ*, and *trkJ-lacZ* fusions on the chromosome, the fragments containing the 5′ end of each open reading frame were amplified by PCR from the genomic DNA of the WT strain using the primer pairs listed in Table 2 and cloned into a suicide vector, pTA-MTL (30), which carries a promoterless *lacZ* gene flanked by terminator sequences. The resulting plasmids were conjugated into the WT strain and its derivative mutant strains via *E. coli* S17-1(λpir), with selection for kanamycin resistance.

Plant growth and bacterial inoculation for nodule formation. *S. rostrata* stems were inoculated with *A. caulinodans* strains, as described previously (31), and then grown at 30°C under a 24-h light

TABLE 1 Bacterial strains and plasmids used in this study

Strain or plasmid	Description	Source or reference
Strains		
A. caulinodans		
ORS571	WT	1
Anx3	Δ*kup*	This study
Anx101	Δ*kdpA*	This study
Anx104	Δ*trkA* Δ*trkI* Δ*trkJ*	This study
Anx105	Δ*kup* Δ*trkJ*	This study
Anx106	Δ*kdpA* Δ*trkA* Δ*trkI* Δ*trkJ*	This study
Anx107	Δ*kup* Δ*trkA* Δ*trkI* Δ*trkJ*	This study
Anx108	Δ*kup* Δ*kdpA*	This study
Anx191	Δ*kup* Δ*trkA*	This study
Anx192	Δ*kup* Δ*trkI*	This study
Anx193	Δ*kup* Δ*trkA* Δ*trkI*	This study
Anx194	Δ*kup* Δ*trkA* Δ*trkJ*	This study
Anx195	Δ*kup* Δ*trkI* Δ*trkJ*	This study
Anx112	Δ*kup* Δ*kdpA* Δ*trkJ*	This study
Anx124	WT *kup-lacZ*	This study
Anx138	WT *kdpF-lacZ*	This study
Anx126	WT *trkA-lacZ*	This study
Anx127	WT *trkJ-lacZ*	This study
Anx139	Δ*kup kdpF-lacZ*	This study
Anx197	Δ*kup* Δ*trkA kdpF-lacZ*	This study
Anx198	Δ*kup* Δ*trkI kdpF-lacZ*	This study
Anx199	Δ*kup* Δ*trkA* Δ*trkI kdpF-lacZ*	This study
Anx200	Δ*kup* Δ*trkJ kdpF-lacZ*	This study
Anx201	Δ*kup* Δ*trkA* Δ*trkJ kdpF-lacZ*	This study
Anx202	Δ*kup* Δ*trkI* Δ*trkJ kdpF-lacZ*	This study
Anx141	Δ*kup* Δ*trkA* Δ*trkI* Δ*trkJ kdpF-lacZ*	This study
Anx114	Δ*trkJ kdpF-lacZ*	This study
E. coli		
DH5α	F^- ϕ80Δ*lacZ*ΔM15 Δ(*lacZYA-argF*)*U169 recA endA hsdR supE44 thi gyrA relA1*	36
S17-1(λpir)	F^- *ompT hsdS*$_B$(r_B^- m_B^-) *gal dcm*(DE3) Δ(*srl-recA*)*306*::Tn*10* (Tet^r)	29
Plasmids		
pK18*mobsacB*	Suicide vector for gene disruption	28
pTA-MTL	Suicide vector for *lacZ* fusion	30
pTAC3	pK18*mobsacB* carrying *kup* deletion fragment	This study
pTAC39	pK18*mobsacB* carrying *kdpA* deletion fragment	This study
pTAC110	pK18*mobsacB* carrying *trkA* deletion fragment	This study
pTAC111	pK18*mobsacB* carrying *trkI* deletion fragment	This study
pTAC40	pK18*mobsacB* carrying *trkAI* deletion fragment	This study
pTAC41	pK18*mobsacB* carrying *trkJ* deletion fragment	This study
pTAC54	pTA-MTL carrying *kup-lacZ* fusion	This study
pTAC58	pTA-MTL carrying *kdpF-lacZ* fusion	This study
pTAC56	pTA-MTL carrying *trkA-lacZ* fusion	This study
pTAC57	pTA-MTL carrying *trkJ-lacZ* fusion	This study

regimen. ARA measurements and optical microscopy observations of stem nodules were carried out as described previously (31).

RT-PCR analysis. Total RNA was isolated from bacterial cultures, and cDNA was synthesized according to previously described methods (31). Subsequent PCRs were performed using the cDNAs and WT genomic DNA (1×10^{-1} ng μl^{-1}) as the templates with the gene-specific primer pairs listed in Table 2.

***β*-Galactosidase activity in the free-living state.** Bacterial cells were suspended in 2 ml of synthetic medium supplemented with 0.05, 0.5, or 5 mM KCl at an optical density at 600 nm (OD_{600}) of 0.5. Cultures were incubated for 4 h with shaking. After incubation, β-galactosidase activity was measured according to a previously reported method (32), with some modifications, as follows. Bacterial cultures (50 μl) were mixed with 450 μl of Z buffer (60 mM Na_2HPO_4, 40 mM NaH_2PO_4, 10 mM KCl, 1 mM $MgSO_4$) supplemented with 50 mM 2-mercaptoethanol, 0.001% SDS, and 50 μl of chloroform. The mixture was vortexed for 30 s, and 50 μl of *o*-nitrophenyl-β-D-galactoside (ONPG; 4 mg ml^{-1} in Z buffer) was added. After incubation at 25°C, reactions were stopped by adding 250 μl of 1 M Na_2CO_3. The mixtures were centrifuged, and 200 μl of the supernatants was transferred to clear 96-well plates. Subsequently, 200 μl of the bacterial cultures was transferred to clear 96-well plates. The absorbance of the supernatants at

TABLE 2 Primers used in this study

Primer	Sequence	Description of underlined sequence
Plasmid construction		
pTAC3		
Acp16	CGAATTCTGATCCGGCACATTGTCA	EcoRI
Acp17	GTCGAGATTGGTCACCCGCCAGGTGATGAGCGACAG	Complement with Acp18
Acp18	CGGGTGACCAATCTCGAC	
Acp19	GCGGATCCGGATGGGATGACGCTAC	BamHI
pTAC39		
Acp254	AACTGCAGCCTGATCGGGATTGAACG	PstI
Acp192	ACGATGTAGGCGAAGCGGAGCGTGTAGCCGATCCAG	Complement with Acp193
Acp193	CCGCTTCGCCTACATCGT	
Acp255	GCTCTAGAGAGGGCGGAGATCTTGGT	XbaI
pTAC110		
Acp198	AACTGCAGAGCGCCTGCTGATTCTC	PstI
Acp579	GCAGGCCACCATGTTCAC	
Acp584	GTGAACATGGTGGCCTGCGTCAGCCTCGAATTCTTCTGA	Complement with Acp579
Acp585	GCTCTAGATGGCTTCCACCGTCTC	XbaI
pTAC111		
Acp586	AACTGCAGTCAGCCTCGAATTCTTCTGA	PstI
Acp587	CAGGATCAGGCTCTCGCCGATGGCTTCCACCGTCTC	Complement with Acp207
Acp207	GGCGAGAGCCTGATCCTG	
Acp208	GCTCTAGAGGCGAGGTGGATGATGAC	XbaI
pTAC40		
Acp198	AACTGCAGAGCGCCTGCTGATTCTC	PstI
Acp253	CAGGATCAGGCTCTCGCCGCAGGCCACCATGTTCAC	Complement with Acp207
Acp207	GGCGAGAGCCTGATCCTG	
Acp208	GCTCTAGAGGCGAGGTGGATGATGAC	XbaI
pTAC41		
Acp212	CGAATTCGGCCATGTGGAAGAGGTG	EcoRI
Acp213	AACAGACGCACTTCCGGAATGTTCCGCCACAAGAGC	Complement with Acp214
Acp214	TCCGGAAGTGCGTCTGTT	
Acp215	GCGGATCCCGTCATCCGCATATCGT	BamHI
pTAC54		
Acp256	GCGGATCCACAAGAAGCGCATCATCCTT	BamHI
Acp285	AACTGCAGAAGATACCAGCGCAGACC	PstI
pTAC58		
Acp307	AACTGCAGCAAGTCCATCTCCTCCTCCA	PstI
Acp308	GCTCTAGAATCATCACGCGCTCCTTC	XbaI
pTAC56		
Acp198	AACTGCAGAGCGCCTGCTGATTCTC	PstI
Acp287	GCTCTAGAGCAGGCCACCATGTTCAC	XbaI
pTAC57		
Acp212	CGAATTCGGCCATGTGGAAGAGGTG	EcoRI
Acp288	GCGGATCCATGTTCCGCCACAAGAGC	BamHI
RT-PCR		
kup		
P1	AGATCGAGCTCTGGACGAAG	
P2	TATTTGACGGTGACGGAAAG	
P3	CACAGCAACCGTGAACGAC	
P4	TTCACCGGATAACCGATCTC	
P5	CGGGTGACCAATCTCGAC	
P6	ATAAATCCCAAGCCATGCAG	
kdpFABC		
P7	GACCGAGATCTCCACCAAGA	

(Continued on next page)

TABLE 2 (Continued)

Primer	Sequence	Description of underlined sequence
P8	GCAGGATGTAGAGGGTCGAA	
P9	CTCGCCGCTTATCTCCTCAC	
P10	GAGATCACGGATGAACAGCA	
P11	CCGCTTCGCCTACATCGT	
P12	AGGAATTGGCGGCATCATAG	
P13	GCCATCACCCTTCTGGTG	
P14	ATGTCGAATTCAGGGACGAG	
trkAI		
P15	TCGACCTCATCTCTCAGACG	
P16	GATTGCTCTCCACCACCTTG	
P17	AGAACGACGTCTCCATCGTC	
P18	GGCGAGGTGGATGATGAC	
P19	GGCGAGAGCCTGATCCTG	
P20	GAGGTGGATGATGACGAAGG	
trkJ		
P21	TCTGGGCCTATACGATCGAG	
P22	TGAAGACGATGGCCACATAG	
P23	GCTGTTCGAGAGCATGTCC	
P24	GCTCGCCACATAAAGGAAGA	
P25	TCCGGAAGTGCGTCTGTT	
P26	GCGAAGAGCAGAAGGAGATG	

415 and 540 nm and the OD_{595} of the cultures were measured using a 96-well microplate reader (680 XR; Bio-Rad, Hercules, CA, USA).

***β*-Galactosidase activity in the symbiotic state.** Stem nodules were longitudinally cut into 3 pieces with a razor blade. The middle piece of each sample was incubated in ice-cold 90% acetone for 15 min and washed with 50 mM phosphate buffer (pH 7.2). The samples were incubated at 25°C in reaction buffer containing 50 mM phosphate buffer (pH 7.0), 0.5 mM $K_3[Fe(CN)_6]$, 0.5 mM $K_4[Fe(CN)_6]$, and 0.05% Triton X-100 with 0.25 mg ml^{-1} X-Gal under vacuum conditions for 30 min, followed by incubation for 3 h under nonvacuum conditions.

Cytoplasmic K^+ content and growth test. For measurements of cytoplasmic K^+ content, bacterial cells were suspended in 10 ml of synthetic medium supplemented with 0.05, 0.5, or 5 mM KCl to an OD_{600} of 1.0. Cultures were incubated for 4 h with shaking. After incubation, the cultures were washed with 50 mM NaCl and suspended in 10 ml of pure water. The OD_{595} of each solution (200 μl) was measured using the 96-well microplate reader. The tubes were then boiled for 30 min, and the cultures were centrifuged. The K^+ content of the supernatant was measured using an atomic absorption spectrophotometer (AA-6200; Shimadzu, Kyoto, Japan) and divided by the OD_{595} of the bacterial strain measured before the disruption of the cells. For the growth tests, bacterial cells were suspended in 2 ml of synthetic medium with KCl to an OD_{600} of 0.05. Cultures were incubated for 16 h with shaking. After incubation, 200 μl of the bacterial cultures was transferred to clear 96-well plates, and the OD_{595} of each culture was measured using the 96-well microplate reader.

Sequence analysis. The nucleotide sequence of the entire genome of *A. caulinodans* ORS571 is available in the DDBJ/EMBL/GenBank databases under accession no. AP009384. Homology searches based on amino acid sequences were performed using the BLASTp program on the National Center for Biotechnology Information (NCBI) server (www.ncbi.nlm.nih.gov/BLAST/). Phylogenetic analyses were carried out using the MUSCLE programs (33) on MEGA5 software (34). Predictions of transmembrane regions on the amino acid sequences were performed using the SOSUI program (35) on the SOSUI server (http://harrier.nagahama-i-bio.ac.jp/sosui/).

SUPPLEMENTAL MATERIAL

Supplemental material for this article may be found at https://doi.org/10.1128/AEM.01197-17.

SUPPLEMENTAL FILE 1, PDF file, 1.8 MB.

SUPPLEMENTAL FILE 2, XLS file, 0.2 MB.

ACKNOWLEDGMENTS

We thank Rio Yoguchi for technical assistance.

This study was supported by the Japan Society for the Promotion of Science (JSPS) (20780231 and 25450081).

The authors declare they have no conflicts of interest.

REFERENCES

1. Dreyfus B, Garcia JL, Gillis M. 1988. Characterization of *Azorhizobium caulinodans* gen. nov., sp. nov., a stem-nodulating nitrogen-fixing bacterium isolated from *Sesbania rostrata*. Int J Syst Bacteriol 38:89–98. https://doi.org/10.1099/00207713-38-1-89.
2. Dreyfus BL, Elmerich C, Dommergues Y. 1983. Free-living *Rhizobium* strain able to grow on N_2 as the sole nitrogen source. Appl Environ Microbiol 45:711–713.
3. Dreyfus B, Dommergues Y. 1981. Nitrogen-fixing nodules induced by *Rhizobium* on the stem of the tropical legume *Sesbania rostrata*. FEMS Microbiol Lett 10:313–317. https://doi.org/10.1111/j.1574-6968.1981.tb06262.x.
4. Suzuki S, Aono T, Lee K-B, Suzuki T, Liu C-T, Miwa H, Wakao S, Iki T, Oyaizu H. 2007. Rhizobial factors required for stem nodule maturation and maintenance in *Sesbania rostrata-Azorhizobium caulinodans* ORS571 symbiosis. Appl Environ Microbiol 73:6650–6659. https://doi.org/10.1128/AEM.01514-07.
5. Epstein W. 2003. The roles and regulation of potassium in bacteria. Prog Nucleic Acid Res Mol Biol 75:293–320. https://doi.org/10.1016/S0079-6603(03)75008-9.
6. Dominguez-Ferreras A, Munoz S, Olivares J, Soto MJ, Sanjuan J. 2009. Role of potassium uptake systems in *Sinorhizobium meliloti* osmoadaptation and symbiotic performance. J Bacteriol 191:2133–2143. https://doi.org/10.1128/JB.01567-08.
7. Sleator RD, Hill C. 2002. Bacterial osmoadaptation: the role of osmolytes in bacterial stress and virulence. FEMS Microbiol Rev 26:49–71. https://doi.org/10.1111/j.1574-6976.2002.tb00598.x.
8. Dosch DC, Helmer GL, Sutton SH, Salvacion FF, Epstein W. 1991. Genetic analysis of potassium transport loci in *Escherichia coli*: evidence for three constitutive systems mediating uptake potassium. J Bacteriol 173:687–696. https://doi.org/10.1128/jb.173.2.687-696.1991.
9. Johnson HA, Hampton E, Lesley SA. 2009. The *Thermotoga maritima* Trk potassium transporter—from frameshift to function. J Bacteriol 191:2276–2284. https://doi.org/10.1128/JB.01367-08.
10. Schlösser A, Meldorf M, Stumpe S, Bakker EP, Epstein W. 1995. TrkH and its homolog, TrkG, determine the specificity and kinetics of cation transport by the Trk system of *Escherichia coli*. J Bacteriol 177:1908–1910. https://doi.org/10.1128/jb.177.7.1908-1910.1995.
11. Schleyer M, Bakker EP. 1993. Nucleotide sequence and 3′-end deletion studies indicate that the K^+-uptake protein Kup from *Escherichia coli* is composed of a hydrophobic core linked to a large and partially essential hydrophilic C terminus. J Bacteriol 175:6925–6931. https://doi.org/10.1128/jb.175.21.6925-6931.1993.
12. Rhoads DB, Waters FB, Epstein W. 1976. Cation transport in *Escherichia coli*. VIII. Potassium transport mutants. J Gen Physiol 67:325–341. https://doi.org/10.1085/jgp.67.3.325.
13. Buurman ET, Kim KT, Epstein W. 1995. Genetic evidence for two sequentially occupied K^+ binding sites in the Kdp transport ATPase. J Biol Chem 270:6678–6685. https://doi.org/10.1074/jbc.270.12.6678.
14. Gaßel M, Siebers A, Epstein W, Altendorf K. 1998. Assembly of the Kdp complex, the multi-subunit K^+-transport ATPase of *Escherichia coli*. Biochim Biophys Acta 1415:77–84. https://doi.org/10.1016/S0005-2736(98)00179-5.
15. Laimins LA, Rhoads DB, Altendorf K, Epstein W. 1978. Identification of the structural proteins of an ATP-driven potassium transport system in *Escherichia coli*. Proc Natl Acad Sci U S A 75:3216–3219. https://doi.org/10.1073/pnas.75.7.3216.
16. Siebers A, Kollmann R, Dirkes G, Altendorf K. 1992. Rapid, high yield purification and characterization of the K^+-translocating Kdp-ATPase from *Escherichia coli*. J Biol Chem 267:12717–12721.
17. Altendorf K, Gassel M, Puppe W, Möllenkamp T, Zeeck A, Boddien C, Fendler K, Bamberg E, Dröse S. 1998. Structure and function of the Kdp-ATPase of *Escherichia coli*. Acta Physiol Scand Suppl 643:137–146.
18. Gaßel M, Möllenkamp T, Puppe W, Altendorf K. 1999. The KdpF subunit is part of the K^+-translocating Kdp complex of *Escherichia coli* and is responsible for stabilization of the complex *in vitro*. J Biol Chem 274:37901–37907. https://doi.org/10.1074/jbc.274.53.37901.
19. Walderhaug MO, Polarek JW, Voelkner P, Daniel JM, Hesse JE, Altendorf K, Epstein W. 1992. KdpD and KdpE, proteins that control expression of the *kdpABC* operon, are members of the two-component sensor-effector class of regulators. J Bacteriol 174:2152–2159. https://doi.org/10.1128/jb.174.7.2152-2159.1992.
20. Kraegeloh A, Amendt B, Kunte HJ. 2005. Potassium transport in a halophilic member of the bacteria domain: identification and characterization of the K^+ uptake systems TrkH and TrkI from *Halomonas elongata* DSM 2581T. J Bacteriol 187:1036–1043. https://doi.org/10.1128/JB.187.3.1036-1043.2005.
21. Zimmann P, Puppe W, Altendorf K. 1995. Membrane topology analysis of the sensor kinase KdpD of *Escherichia coli*. J Biol Chem 270:28282–28288. https://doi.org/10.1074/jbc.270.47.28282.
22. Rothenbücher MC, Facey SJ, Kiefer D, Kossmann M, Kuhn A. 2006. The cytoplasmic C-terminal domain of the *Escherichia coli* KdpD protein functions as a K^+ sensor. J Bacteriol 188:1950–1958. https://doi.org/10.1128/JB.188.5.1950-1958.2006.
23. Laermann V, Ćudić E, Kipschull K, Zimmann P, Altendorf K. 2013. The sensor kinase KdpD of *Escherichia coli* senses external K. Mol Microbiol 88:1194–1204. https://doi.org/10.1111/mmi.12251.
24. Lee C-R, Cho S-H, Yoon M-J, Peterkofsky A, Seok Y-J. 2007. *Escherichia coli* enzyme IIA^{Ntr} regulates the K^+ transporter TrkA. Proc Natl Acad Sci U S A 104:4124–4129. https://doi.org/10.1073/pnas.0609897104.
25. Lüttmann D, Heermann R, Zimmer B, Hillmann A, Rampp IS, Jung K, Görke B. 2009. Stimulation of the potassium sensor KdpD kinase activity by interaction with the phosphotransferase protein IIA^{Ntr} in *Escherichia coli*. Mol Microbiol 72:978–994. https://doi.org/10.1111/j.1365-2958.2009.06704.x.
26. Beringer JE. 1974. R factor transfer in *Rhizobium leguminosarum*. J Gen Microbiol 84:188–198.
27. Horton RM, Cai ZL, Ho SN, Pease LR. 1990. Gene splicing by overlap extension: tailor-made genes using the polymerase chain reaction. Biotechniques 8:528–535.
28. Schäfer A, Tauch A, Jäger W, Kalinowski J, Thierbach G, Pühler A. 1994. Small mobilizable multi-purpose cloning vectors derived from the *Escherichia coli* plasmids pk18 and pk19: selection of defined deletions in the chromosome of *Corynebacterium glutamicum*. Gene 145:69–73. https://doi.org/10.1016/0378-1119(94)90324-7.
29. Simon R, Priefer U, Pühler A. 1983. A broad host range mobilization system for *in vivo* genetic engineering: transposon mutagenesis in Gram negative bacteria. Nat Biotechnol 1:784–791. https://doi.org/10.1038/nbt1183-784.
30. Iki T, Aono T, Oyaizu H. 2007. Evidence for functional differentiation of duplicated *nifH* genes in *Azorhizobium caulinodans*. FEMS Microbiol Lett 274:173–179. https://doi.org/10.1111/j.1574-6968.2007.00823.x.
31. Nakajima A, Aono T, Tsukada S, Siarot L, Ogawa T, Oyaizu H. 2012. Lon protease of *Azorhizobium caulinodans* ORS571 is required for suppression of *reb* gene expression. Appl Environ Microbiol 78:6251–6261. https://doi.org/10.1128/AEM.01039-12.
32. Miller JH. 1972. Experiments in molecular genetics. Cold Spring Harbor Laboratory, Cold Spring Harbor, NY.
33. Edgar RC. 2004. MUSCLE: multiple sequence alignment with high accuracy and high throughput. Nucleic Acids Res 32:1792–1797. https://doi.org/10.1093/nar/gkh340.
34. Tamura K, Peterson D, Peterson N, Stecher G, Nei M, Kumar S. 2011. MEGA5: molecular evolutionary genetics analysis using maximum likelihood, evolutionary distance, and maximum parsimony methods. Mol Biol Evol 28:2731–2739. https://doi.org/10.1093/molbev/msr121.
35. Hirokawa T, Boon-Chieng S, Mitaku S. 1998. SOSUI: classification and secondary structure prediction system for membrane proteins. Bioinformatics 14:378–379. https://doi.org/10.1093/bioinformatics/14.4.378.
36. Grant SG, Jessee J, Bloom FR, Hanahan D. 1990. Differential plasmid rescue from transgenic mouse DNAs into *Escherichia coli* methylation-restriction mutants. Proc Natl Acad Sci U S A 87:4645–4649. https://doi.org/10.1073/pnas.87.12.4645.